Using a Fast Fourier method to model sound propagation in a stratified atmosphere over a stratified porous-elastic ground

S. Tooms and K. Attenborough,
The Open University,
Milton Keynes,
England.

Abstract

Using a Fast Fourier integration method and a global matrix method for solution of the boundary condition equations at all interfaces simultaneously, a useful tool for predicting acoustic propagation in a stratified fluid over a stratified porous-elastic solid has been developed. The model for the solid is a modified Biot-Stoll model incorporating four parameters describing the pore structure corresponding to the Rayleigh-Attenborough rigid-porous structure model.

The method is also compared to another Fast Fourier code (CERL-FFP) which models the ground as an impedance surface under a horizontally stratified air. Agreement with the CERL FFP is good.

The effects on sound propagation of a combination of ground elasticity, complex ground structure, and atmospheric conditions are demonstrated by theoretical results over a snow layer, and experimental results over a model ground surface.

Introduction

The ground has conventionally been modelled for outdoor sound propagation as either an impedance surface or a rigid-porous structure. These approaches have both been highly productive in the case of high density materials. However in reality the ground is poro-elastic. Ground surfaces have hitherto been modelled as such when the interest has been in acoustic to seismic coupling, but there has been little interest in porous-elastic ground models in propagation in the air. For some outdoor ground surfaces (such as snow or forest floors for example) the bulk density of the material is low enough for seismic effects to become important for sound propagation over the surface at some frequencies.

In this paper an FFP propagation model is used to calculate sound pressure levels over a porous-elastic ground surface. The model's predictions are compared to the predictions of other propagation models for the high density, high seismic velocity rigid-porous limit of the porous-elastic ground model. The effects on acoustic propagation of the elasticity of various ground surfaces is then shown by comparison to the rigid frame limit. Using a multiply layered fluid atmosphere the combined effects of meteorology and ground elasticity are examined.

The Biot-Stoll poro-elastic model

The ground model used in this investigation was a modified Biot-Stoll Poro-Elastic model[1,2,3]. Propagation within the material is via three different modes; a fast wave, equivalent to the seismic P wave: a slow wave equivalent to the pore wave in the Rayleigh Attenborough rigid-porous model[4]: and a shear wave equivalent to the seismic S wave. Each wavetype causes vibration in both the solid material and the pore fluid. Attenuation of all three wavetypes is predicted by the theory due to viscous losses on the

pore walls, though it has been shown to underpredict the attenuation in real materials because other loss mechanisms are not taken into account. Hence an extra attenuation is added as an imaginary part of the fast and shear propagation constants.

The Fast Fourier Method

If one applies a Hankel transform in range to the Helmholtz equation one obtains the depth separated wave equation:

$$\left(\frac{d^2}{dz^2} + \left(k^2 - k_m^2(z)\right)\right)\Gamma(k,z) = \bar{h}(k,z), \tag{1}$$

where, for a point source,

$$\bar{h}(k,z) = \frac{1}{2\pi}\delta(z - z_0) \tag{2}$$

Solutions to this equation are depth dependent only and are equivalent to solutions to the wave equation for continuous plane wave incidence. In order to obtain a range dependent solution one must obtain depth dependent solutions to the depth separated wave equation, and then perform the inverse Hankel Transform on the solution to equation 1 , which is in terms of horizontal wavenumber.

The exact range dependent solution is in the form;

$$F_{(x,d)} = \int_{k_h=0}^{\infty} J_\nu(k_h.x).\Gamma(k_h,d).dk_h, \tag{3}$$

where Γ is the depth dependent Greens function.

A large argument approximation to the Bessel function [5] is:

$$J_\nu(z) \simeq \frac{1}{\sqrt{2\pi z}}\left[e^{i(z-\pi\nu/2-\pi/4)} + e^{-i(z-\pi\nu/2-\pi/4)}\right] \tag{4}$$

This approximation together with the replacement of the integration by a finite sum gives the approximate equation for $F_{(x,d)}$:

$$F_{(x_m,d)} \simeq \frac{\delta k N^{1/2}}{2\pi m^{1/2}}\left[e^{-i\pi/4}\sum_{n=0}^{N-1}\Gamma_{(k_n,d)}n^{\frac{-1}{2}}e^{\frac{2i\pi mn}{N}} + e^{i\pi/4}\sum_{n=0}^{N-1}\Gamma_{(k_n,d)}n^{\frac{-1}{2}}e^{\frac{-2i\pi mn}{N}}\right]. \tag{5}$$

This Fourier series approximation can then be improved by corrections to allow for the truncation of the integral to infinity to a finite wavenumber, $k_{h(max)}$, and the avoidance of pole(s) on the real axis[6], which together lead to inaccuracies and oscillations in the result, to give

$$\begin{aligned} F_{(x_m,d)} \simeq \frac{\delta k N^{\frac{1}{2}}}{2\pi m^{\frac{1}{2}}}\Bigg[&e^{-i\pi/4}\sum_{n=0}^{N-1}C_{(k_n,d)}e^{\frac{2i\pi mn}{N}}e^{\frac{2\pi m\alpha}{N}} \\ &+ e^{i\pi/4}\sum_{n=0}^{N-1}C_{(k_{N-n},d)}e^{\frac{2i\pi(N-m)n}{N}}e^{\frac{-2\pi m\alpha}{N}}\Bigg]. \end{aligned} \tag{6}$$

where

$$G_{(k_n,d)} = \Gamma_{(k_n,d)} + \frac{iN\Gamma_{(k_0,d)}}{\alpha\Delta}\left[1 - e^{(\Delta(i\alpha-n)/N)}\right], \tag{7}$$

$$C_{(k_n,d)} = G_{(k_n,d)}.(n - i\alpha)^{-1/2} + G_{(k_{N-1},d)}N^{-1/2}S^*, \tag{8}$$

and S^* is an approximation to the sum,

$$S = \sum_{j=1}^{\infty}(j + [(n - i\alpha)/N])^{-1/2}. \tag{9}$$

The Environment

The environment is assumed to be range independent and to consist of a fluid (air) upper half-space overlying a set of horizontal fluid (air) layers of differing sound speeds and densities. The lowest of these fluid layers is in contact with a ground made up of a set of horizontal elastic porous layers under which is an elastic porous half-space. The number of layers in either fluid or ground can be set to zero.

The Depth Dependent Green's function

The depth dependent Green's function Γ must be solved for the above environment.

In a fluid layer containing a spherical point source the depth dependent Green's function is

$$\Gamma = \left[\frac{1}{\beta_0} e^{i.(h_s-h).\beta_0} + R_{\uparrow}.e^{i.(h_1-h).\beta_0} + R_{\downarrow}.e^{i.(h-h_2).\beta_0}\right]. \tag{10}$$

The $R_{\updownarrow}$ are calculated by solution of the boundary condition equations at the interfaces.

In the porous elastic medium there are three scalar displacement potentials describing propagation in the fluid,

$$\Phi_1 = \int_0^\infty \bar{\Phi}_1 J_0(k_h.r).k_h.dk_h \tag{11}$$

$$\Phi_2 = \int_0^\infty \bar{\Phi}_2 J_0(k_h.r).k_h.dk_h \tag{12}$$

$$\Phi_3 = \int_0^\infty \bar{\Phi}_3 J_0(k_h.r).dk_h, \tag{13}$$

Φ_1 is the longitudinal displacement potential in the solid, Φ_2 is the longitudinal displacement potential in the pore fluid, Φ_3 is the transverse displacement potential in the solid, to which the fluid transverse displacement potential is directly proportional.

In a porous-elastic layer, bounded by interfaces at depths d_1 and d_2, in the absence of a source, the $\bar{\Phi}_i$s at a depth z are given by.

$$\bar{\Phi}_1 = A_{1\downarrow}e^{i(z-d_1)\beta_1} + A_{1\uparrow}e^{i(d_2-z)\beta_1} + A_{2\downarrow}e^{i(z-d_1)\beta_2} + A_{2\uparrow}e^{i(d_2-z)\beta_2} \ , \tag{14}$$

$$\bar{\Phi}_2 = m_1\left(A_{1\downarrow}e^{i(z-d_1)\beta_1} + A_{1\uparrow}e^{i(d_2-z)\beta_1}\right) + m_2\left(A_{2\downarrow}e^{i(z-d_1)\beta_2} + A_{2\uparrow}e^{i(d_2-z)\beta_2}\right) \ , \tag{15}$$

$$\bar{\Phi}_3 = A_{3\downarrow}e^{i(z-d_1)\beta_3} + A_{3\uparrow}e^{i(d_2-z)\beta_3} \ , \tag{16}$$

The m_i are the ratios of the amplitude in the solid and pore fluid for each wavetype, and the $\beta_i = (k_i^2 - k^2)^{1/2}$, where the k_i are propagation constants, and k is the horizontal wavenumber. The depth dependent Green's function Γ for a desired output parameter in the fluid is a function of the $\bar{\Phi}_i$. The $A_{\updownarrow}$ are calculated by solution of the boundary condition equations.

Boundary conditions

Boundary condition equations in cylindrical polar coordinates (r, θ, z) are needed. However the axisymmetric nature of the problem considered here means that there is no θ dependence.

At boundaries between two fluid layers the two boundary conditions are

1. continuity of pressure,
2. continuity of normal particle displacement,

At the interface between the fluid and the porous elastic medium there are four boundary conditions,

1. continuity of total normal stress[3],
2. continuity of normal displacement[3],
3. continuity of fluid pressure[7],
4. continuity of tangential stress,

Six boundary conditions are required at each interface between porous-elastic layers. These boundary conditions are the four above and two others,

5. continuity of normal relative fluid displacement, and
6. continuity of tangential frame displacement.

The range dependent parts of the boundary condition equations are identical on each side of the boundary, therefore only the depth dependent Green's functions of the boundary conditions need to be equated.

The boundary condition equations are solved simultanaeously for the $A_\updownarrow$ and $R_\updownarrow$ at all interfaces. The depth dependent Green's function is then calculated for the desired output parameter (sound pressure level, frame displacement, etc). The range dependent solution is calculated using the FFP method described above.

Comparison to other propagation models

For propagation above a rigid-porous halfspace the model compares well with other propagation models, such as the CERL-FFP (see figure 1)[8], and Attenborough, Hayek, and Lawther's 'exact' analytic model(see figure 2)[7]. Above an extended reaction rigid-porous layer over a non-porous backing agreement with Nicholas-Berry and Daigle's propagation model is good for a wide variety of model surfaces(see figures 3 and 4) [9]. Source and receiver heights are 0.5 and 0.3 metres respectively.

Effects of ground surface elasticity on sound propagation

The largest effects of ground elasticity on sound propagation over it are likely to be where the bulk density of the ground surface is small. The most common ground cover where this is so is a snow layer. Measured normal surface impedance over snow cover sometimes shows low frequency peaks [10,11]. These could be interpreted as seismic resonances in a snow layer. Figure 5 shows the predicted excess attenuation over an 8cm thick snow layer overlying a rigid nonporous halfspace at twenty metres range, using a rigid-porous model, and porous-elastic model. The pore structure and elastic parameters are taken calculated from Sommerfeld[12], Johnson[11] Ishida[10] and Attenborough and Buser[13]. A resonant effect can clearly be seen at about 810Hz in the porous elastic model output which is not present for the rigid-porous model. Figure 6 shows the predicted excess attenuation over the same snow layer at 810Hz as a function of range. This figure demontrates that at this frequency a seismic resonance in the snow layer leads to an apparent hardening of the snow surface at a short range, leading to less attenuation due to ground absorption. The behaviour at longer ranges shows that away from the source the attenuation due to the ground is unaffected by the elastic effects, but the signal amplitude is increased due to the reduced attenuation near to the source.

Combined effects of elasticity and atmospheric sound velocity gradients

Continuous sound velocity gradients can be modelled by thin homogeneous layers as long as the layer thickness is much less than the wavelength of the sound [14]. In figure 7 the combined effect of the logarithmic downward refracting sound velocity gradient(roughness length 5.10^{-3}metres, temperature difference between ground and 4.0 metres 7° Centigrade) and an elastic surface are shown. The difference between elastic and rigid models remains approximately the same as for no gradient.

Comparison with experiments

In order to test the validity of this porous-elastic propagation model, measurements of the level difference between two vertically separated microphones were made over a thin (4cm) layer of low density foam material. The foam was attached to a non-porous concrete surface. A point noise source was suspended over the foam surface.

The elastic and porous parameters of the foam were separately measured using non-acoustic techniques. The measured level difference was compared to the level difference predicted using both rigid and poro-elastic models. The results are shown in figure 8. The geometry used for this figure was source height 0.2 metres, receiver heights 0.01 and 0.2 metres, and range 0.4 metres. The results show a better agreement with the elastic model than with the rigid model.

Conclusions

An FFP model for propagation over porous-elastic surfaces has been developed. It has been shown that in the rigid frame limit it agrees well with other propagation models. For sound propagation over low bulk density layered materials it has been shown that ground elasticity can have a substantial effect on received sound pressure levels for both real and theoretical results.

Table 1: Material parameters used in the prediction of excess attenuation

Parameter	Unit	Rigid-porous Halfspace	Rigid-porous layer	Snow layer	Foam layer
Flow resistivity σ	MKSraylsm^{-1}	100000	10000	15900	18400
Porosity Ω	-	0.3	0.3	0.804	0.97
Pore shape factor ratio s_p	-	0.5	0.5	0.5	0.5
Grain shape factor n'	-	0.5	0.5	0.5	63.8
Bulk density	kgm^{-3}	-	-	184.0	32.0
P-wave velocity v_p	ms^{-1}	-	-	130.0	79.0
S-wave velocity v_s	ms^{-1}	-	-	90.0	56.0
$\Im(v)/\Re(v)$	-	-	-	0.05	0.085
Grain bulk modulus K_r	Nm^{-2}	-	-	1.10^9	1.10^{10}
Layer depth	m	-	0.1	0.08	0.04

References

[1] M.A. Biot. Theory of propagation of elastic waves in a fluid saturated porous solid. *J.Acoust.Soc.Am.*, 168–191, 1956.

[2] M.A. Biot. Mechanics of deformation and acoustic propagation in porous media. *J.Applied Physics*, 33(4):1482–1498, 1962.

[3] J.M. Sabatier, H.E. Bass, L.M. Bolen, K. Attenborough, and V.V.S.S. Sastry. The interaction of airborne sound with the porous ground: the theoretical formulation. *J.Acoust.Soc.Am.*, 79(5):1345–1352, May 1986.

[4] K. Attenborough. On the acoustic slow wave in air filled granular media. *J.Acoust.Soc.Am.*, 81(1):93–102, Jan. 1987.

[5] M.Abramowitz and I.A.Stegun. *Handbook of Mathematical Functions.* Dover NY USA, 1970.

[6] T.L. Richards. Accurate fft-based hankel transforms for prediction of outdoor sound propagation. *J.Sound and Vib.*, 109(1):157–167, 1986.

[7] K.Attenborough, S.I.Hayek, and J.M.Lawther. Propagation of sound above a porous half-space. *J.Acoust.Soc.Am.*, 68(5):1493–1501, November 1980.

[8] S.J.Franke and G.W.Swenson(Jr). A brief tutorial on the fast field program (ffp) as applied to sound propagation in the air. *Applied Acoustics*, 27(3):203–216, September 1989. Univ of Illinois at Urbana-Champaign.

[9] J.Nicholas, J.L.Berry, and G.A.Daigle. Propagation of sound above a finite layer of snow. *J.Acoust.Soc.Am*, 77(1):67–73, 1985.

[10] T. Ishida. Acoustic properties of snow. *Contributions from the Intensity of Low Temperature Science Series A.*, 20:23–63, 1965.

[11] J.B. Johnson. On the application of biot's theory to acoustic wave propagation in snow. *Cold regions Science and Technology*, 6:49–60, 1982.

[12] R A Sommerfeld. A review of snow acoustics. *Reviews of Geophysics and Space Physics*, 20(1):62–66, February 1982.

[13] K.Attenborough and O.Buser. On the application of rigid-porous models to impedance data for snow. *J.Sound Vib.*, 124(2):315–327, 1988.

[14] S.J.Franke, R.Raspet, and C.H.Liu. Numerical predictions of atmospheric sound pressure levels in shadow zones. *J.Acoust.Soc.Am.*, 83(2):816–820, 1988.

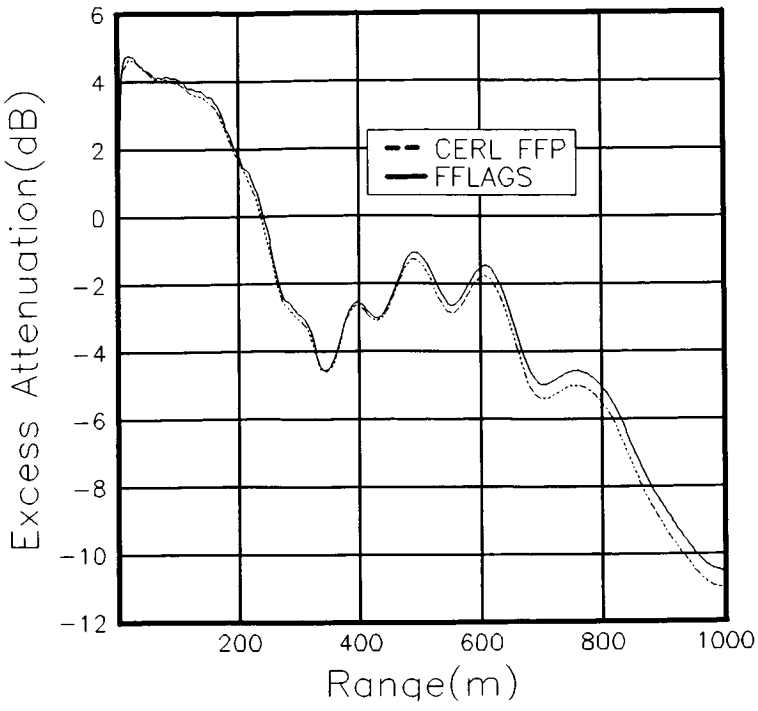

Figure 1 Comparison of CERL FFP and FFLAGS for propagation over a rigid-porous halfspace in a 12 layered atmosphere. Frequency=50Hz.

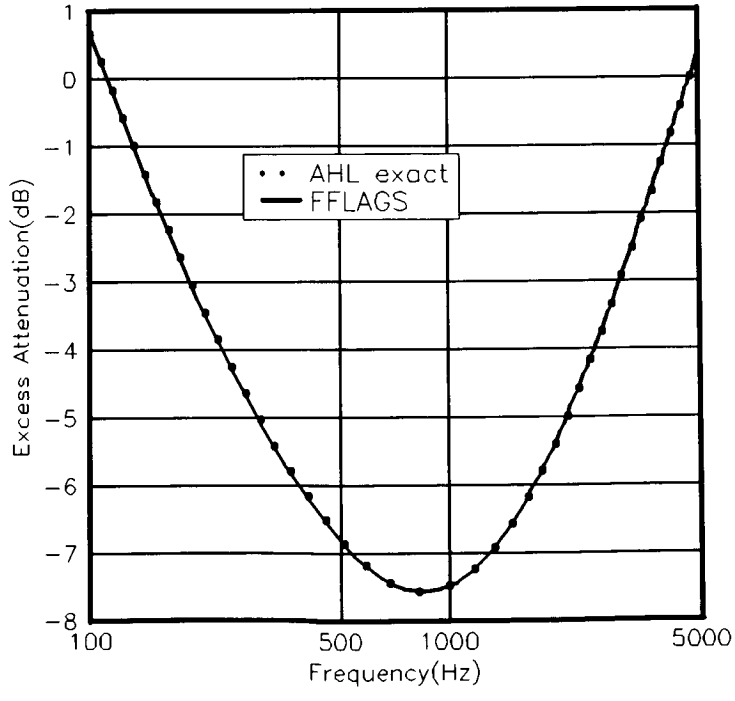

Figure 2 Comparison of FFLAGS to the predictions of Attenborough, Hayek, and Lawther's exact extended reaction model for propagation over an extended reaction rigid-porous halfspace. Range=20 metres.

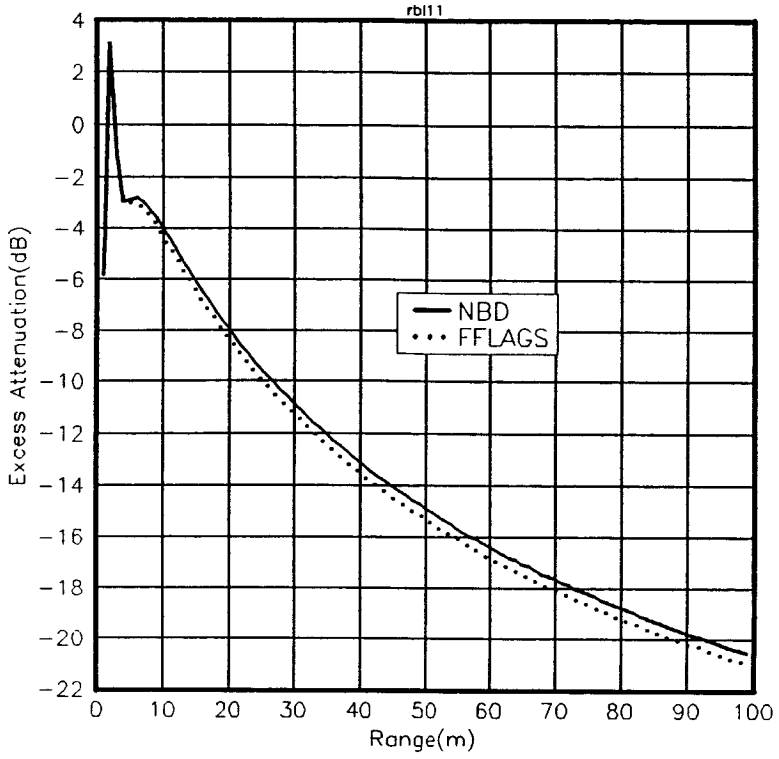

Figure 3 Comparison of Nicholas Berry and Daigle's model for predicted excess attenuation over an extended reaction rigid-backed layer at 100Hz.

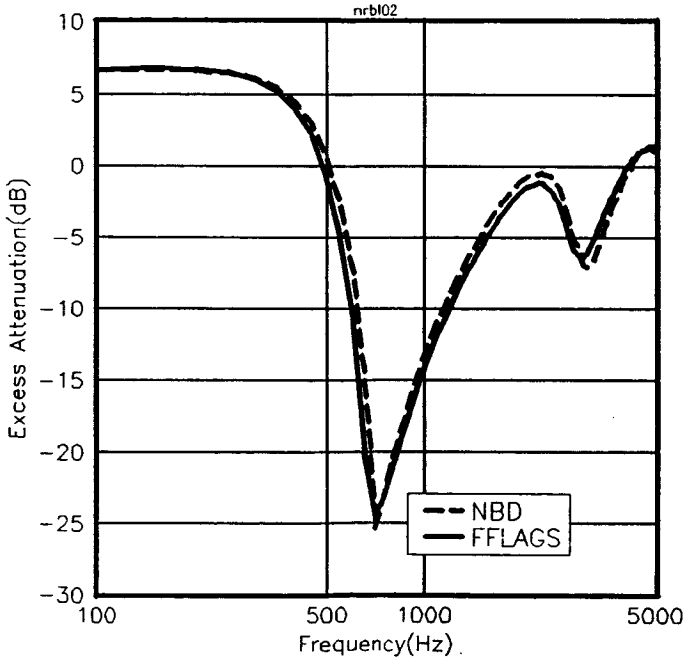

Figure 4 Comparison of FFLAGS to Nicholas Berry and Daigle's model for predicted excess attenuation over an extended reaction rigid backed layer at 20 metres.

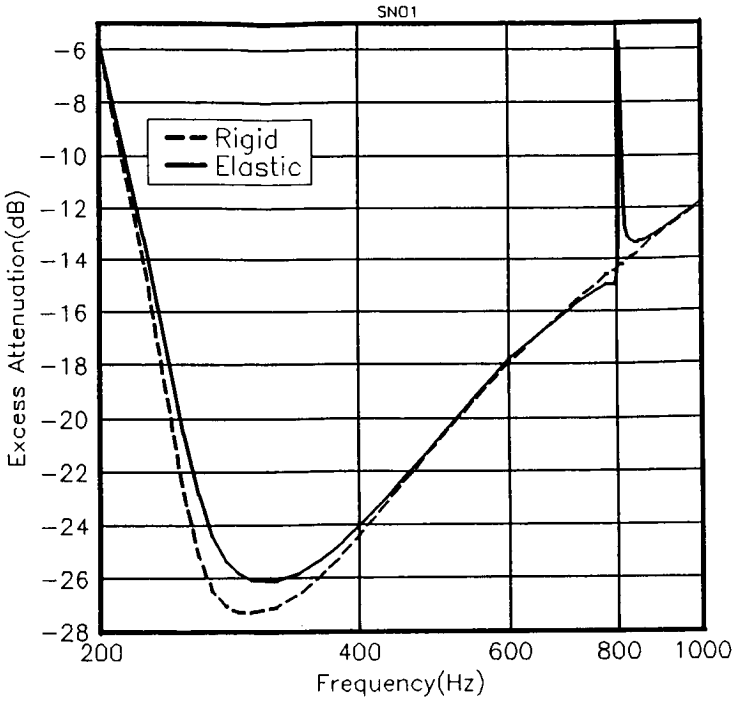

Figure 5 Predicted excess attenuation over thin snow layer using FFLAGS with rigid-porous parameters, and porous-elastic parameters. Range 20 metres.

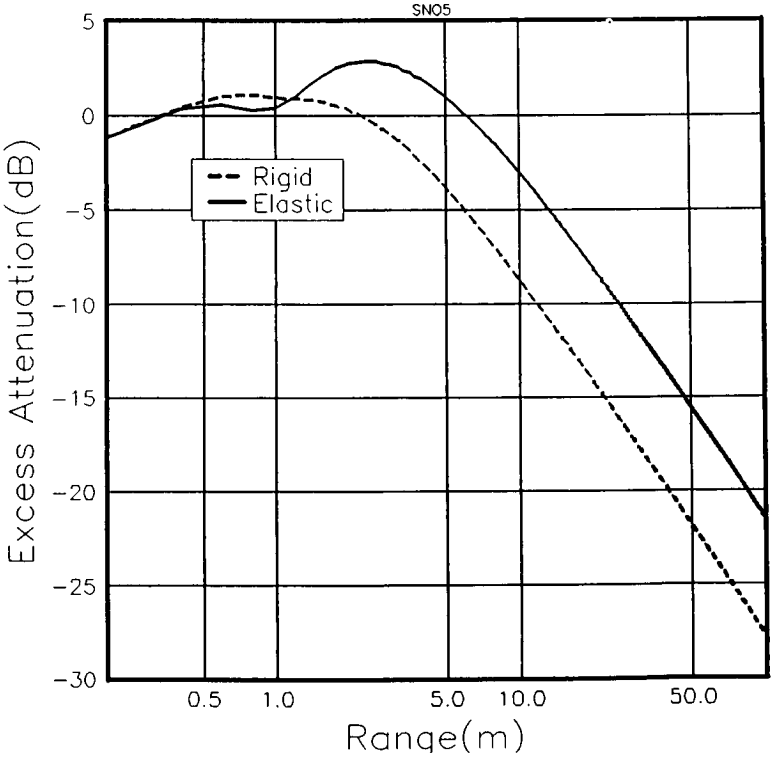

Figure 6 Predicted excess attenuation over thin snow layer at 810Hz. Showing difference between rigid and elastic model at this frequency.

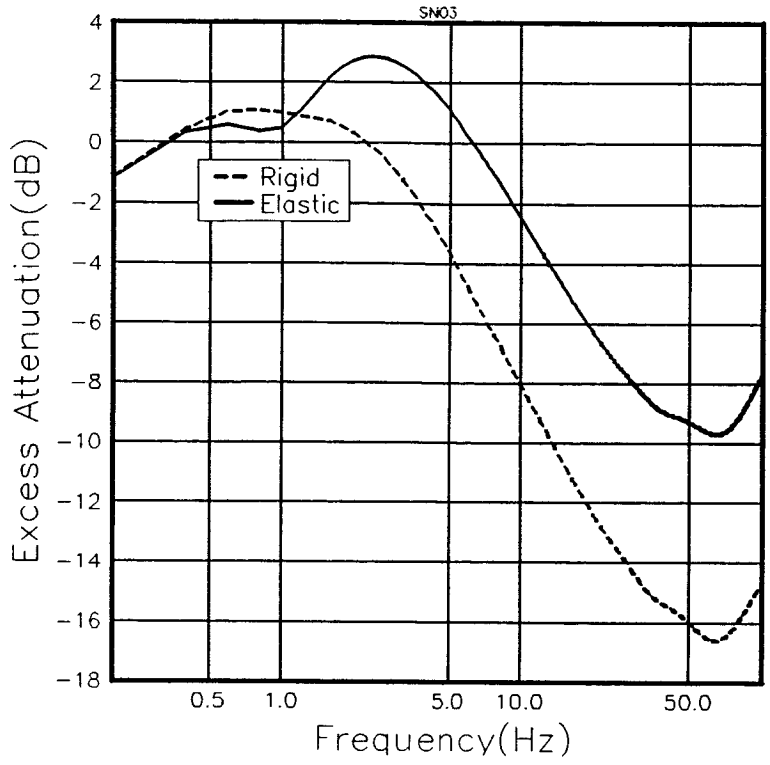

Figure 7 Predicted excess attenuation over thin snow layer at 810Hz in the presence of a downward refracting logarithmic sound velocity gradient.

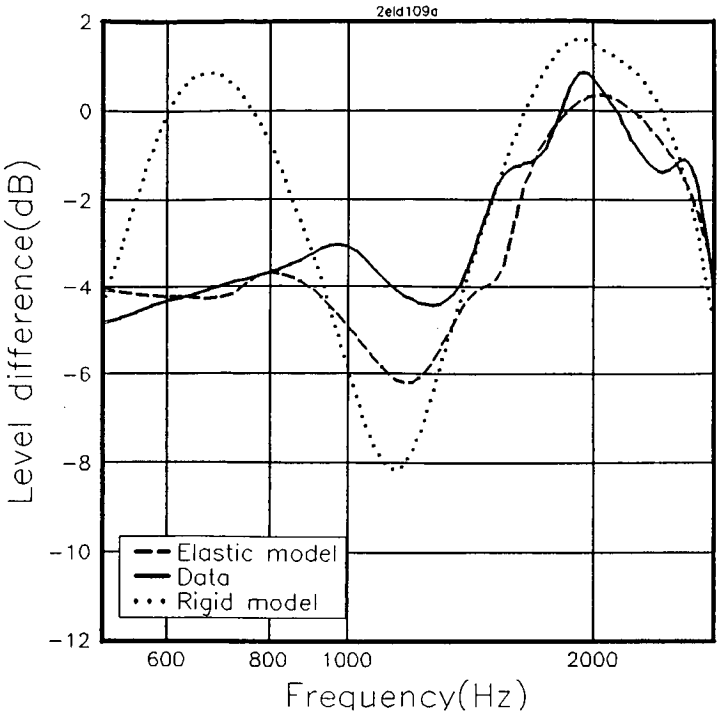

Figure 8 Measured Level difference between two vertically separated microphones (heights 0.2 and 0.01 metres) at a range of 0.4 metres from a point source over a thin (4cm) rigidly backed foam surface. Compared to the predicted level difference using rigid-porous and porous-elastic models, calculated from direct measurement of the pore and elastic parameters of the foam.